Journal of Sound and Vibration (1998) **209**(1), 15–41

THREE-DIMENSIONAL VIBRATIONS OF THICK CIRCULAR AND ANNULAR PLATES

J. SO

Korea Airport Construction Authority, 2172-1, *Woonseo-Dong*, *Joong-Ku*, *Incheon*, *Korea* 400-340

AND

A. W. LEISSA

Applied Mechanics Program, *The Ohio State University*, *Columbus*, *OH* 43210, *U.S.A.*

(*Received* 9 *January* 1997, *and in final form* 16 *July* 1997)

The Ritz method is applied in a three-dimensional (3-D) analysis to obtain accurate frequencies for thick circular and annular plates. The method is formulated in a manner which allows one to have any combination of free or fixed plate boundaries. Admissible functions for the three displacement components are chosen as trigonometric functions in the circumferential co-ordinate, and algebraic polynomials in the radial and axial co-ordinates. Upper bound convergence of the non-dimensional frequencies to at least four significant figures is demonstrated. Comparisons of results are made with ones obtained by others using 2-D Mindlin thick plate theory, and with other 3-D solutions. Extensive and accurate (four significant figure) frequencies are presented for completely free circular plates having thickness-to-diameter ratios of 0·2, 0·3, 0·4 and 0·5 for Poisson's ratios $\nu = 0$, 0·3 and 0·499. Frequencies are also given for thick annular plates having a thickness-to-outer-diameter of 0·2, inside-to-outside-diameter ratios of 0·1, 0·5 and 0·9, and $\nu = 0 \cdot 3$. All 3-D modes are included in the analyses; e.g., flexural thickness-shear, inplane stretching, and torsional. The circular and annular plate frequency data given is *exact* to at least four digits, thus being benchmark data against which results from 2-D thick plate theories or other approximate methods (e.g., finite elements) may be compared.

1. INTRODUCTION

Vibrating plates have tremendous practical importance in the world. Recognizing this importance, more than 2000 papers have been published on the subject of free, undampled vibrations alone, determining natural frequencies. At least 90 per cent of the published results are theoretical, based upon two-dimensional plate theories, either classical thin-plate theory, or theories which consider shear deformation and rotary inertia effects and are thought to be reasonably accurate for thick plates and/or higher frequency modes. However, the accuracies of these can only be assessed when results from them are compared with truly accurate results obtained from three-dimensional (3-D) analysis, where no artificial, kinematic constraints are placed upon the displacements. The present work provides such accurate, 3-D results for two important classes of problems, circular and annular plates, for the only types of edge conditions which can be exactly duplicated in reality—completely free.

In recent papers by the present authors [1–3], a 3-D method of analysis was presented for the free vibrations of solid and hollow cylinders of elastic and isotropic material. The

0022–460X/98/010015 + 27 $25.00/0/sv971228

analysis was based upon the Ritz method using two co-ordinate systems: (1) cylindrical co-ordinates (r, θ, z); and (2) local co-ordinates where θ and z in cylindrical co-ordinates remain the same, but r is measured from the middle of the cylindrical wall. Also, as a general case, 3-D vibrations of truncated hollow cones were investigated [4, 5].

Other 3-D free vibrations of finite circular and hollow cylinders were studied by many researchers. Among them, some investigated the free vibrations of thick circular and annular plates using their own methods [6–9]. Some of their solutions were also compared with those of Mindlin's plate theory [10].

The primary objective of the present work is to present truly accurate values of the free-vibration frequencies of thick circular and annular plates, which are complementary to references [1–3]. In reference [2] accurate frequencies were given for completely free, solid circular cylinders, as well as for ones having one end fixed. For the completely free case, frequencies obtained were exact to four significant figures. However, none of the cylinders may be regarded as plates, for their length-to-diameter (L/D) ratios were $1, 1{\cdot}5, 2, 3$ and 5. The accuracy of 1-D theories for vibrating rods and beams $(L/D = 3, 5, 10, 20, 40)$ was the theme of reference [1]. No comparisons were made for plate-like cylinders. Reference [3] considered hollow circular cylinders. In the present work accurate frequencies are given for plate-like cylinders $(L/D = 0{\cdot}5$ and less). Besides presenting the method of analysis and establishing its accuracy by means of convergence studies, comparisons are made with the other most accurate 3-D results known to date. The accurate 3-D results presented here serve as benchmarks against which other approximate methods (e.g., finite element, finite difference methods) and 2-D plate theories, first order and higher order, may be tested.

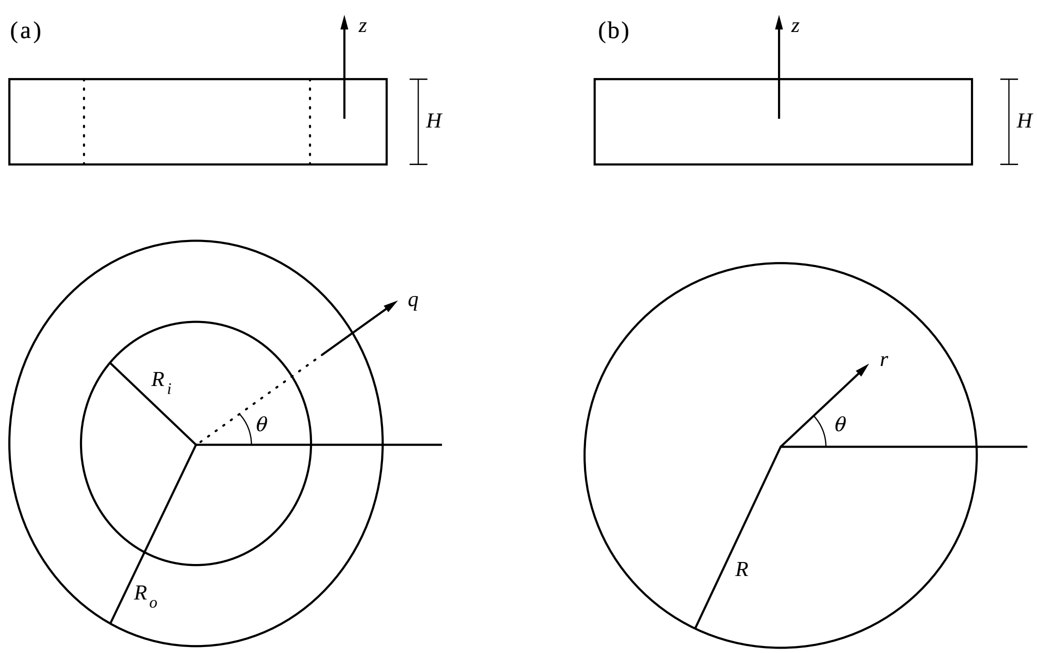

Figure 1. (a) Annular plate with local co-ordinate system (q, θ, z). (b) Circular plate with cylindrical co-ordinate system (r, θ, z).

TABLE 1

Convergence frequencies in $\omega R\sqrt{(\rho/G)}$ for the five lowest axisymmetric ($n = 0$) and ζ-symmetric modes, where $H/D = 0{\cdot}2$ and $\nu = 0{\cdot}3$

I	J	D	1	2	3	4	5
1	1	8	3·44267	10·22177	14·35485	15·94322	20·58867
3	1	16	3·43639	8·62444	11·86034	12·35021	14·37381
5	1	24	3·43639	8·59221	11·56885	12·05093	14·26232
7	1	32	3·43639	8·59200	11·55634	12·04391	13·52930
9	1	40	3·43639	8·59199	11·55615	12·04274	13·47270
10	1	44	3·43639	8·59199	11·55615	12·04251	13·47146
1	2	12	3·44267	10·19499	13·85522	15·61110	17·59332
3	2	24	**3·43638**	8·62002	11·54181	12·12318	13·91331
5	2	36	3·43638	8·58884	11·49409	11·62695	13·88971
7	2	48	3·43638	8·58868	11·49025	11·61245	13·42799
9	2	60	3·43638	8·58868	11·48998	11·61220	13·38522
10	2	66	3·43638	8·58868	11·48995	11·61217	13·38439
1	3	16	3·44267	10·19489	13·84592	15·60478	17·53649
3	3	32	3.43638	8.61992	11.53807	12.12207	13.90757
5	3	48	3·43638	8·58884	11·49182	11·62459	13·88422
7	3	64	3·43638	**8·58867**	11·48816	11·61002	13·42651
9	3	80	3·43638	8·58867	**11·48791**	**11·60977**	**13·38422**
1	4	20	3·44267	10·19489	13·84589	15·60476	17·53607
3	4	40	3·43638	8·61992	11·53806	12·12207	13·90755
5	4	60	3·43638	8·58884	11·49179	11·62456	13·88417
7	4	80	3·43638	8·58867	11·48815	11·61001	13·42635
1	5	24	3·44267	10·19489	13·84589	15·60476	17·53607
3	5	48	3·43638	8·61992	11·53806	12·12207	13·90755
5	5	72	3·43638	8·58884	11·49179	11·62455	13·88417
7	5	96	3·43638	8·58867	11·48815	11·61001	13·42632
1	6	28	3·44267	10·19489	13·84589	15·60476	17·53607
3	6	56	3·43638	8·61992	11·53806	12·12207	13·90755
5	6	84	3·43638	8·58884	11·49179	11·62455	13·88417
6	6	98	3·43638	8·58867	11·49077	11·61356	13·45765

2. ANALYSIS

A representative annular plate of inner diameter D_i ($=2R_i$) and outer diameter D_o ($=2R_o$) and thickness H is shown in Figure 1. In the case of a solid circular plate, the inner diameter vanishes, and thus the diameter D ($=2R$) and the thickness H are the only two geometric parameters.

Cylindrical co-ordinates (r, θ, z), also shown in the figure, are used in the analysis. Location of the co-ordinate origin in the z-direction is chosen at the center of the plate. For convenience, the r and z co-ordinates are made dimensionless as follows:

$$\xi = \frac{r}{R_o}, \qquad \zeta = \frac{z}{H} \tag{1}$$

where R_o is the outer radius of the annular plate (R is used for the solid plate).

Displacement components in the ξ, θ and ζ directions are u, v and w. For the free, undamped vibration, their time response is sinusoidal and, moreover, the circular symmetry of the plate allows the displacement to be expressed by

$$u(\xi, \theta, \zeta, t) = U(\xi, \zeta) \cos n\theta \sin(\omega t + \phi)$$

$$v(\xi, \theta, \zeta, t) = V(\xi, \zeta) \sin n\theta \sin(\omega t + \phi)$$

$$w(\xi, \theta, \zeta, t) = W(\xi, \zeta) \cos n\theta \sin(\omega t + \phi) \tag{2}$$

where ω is a natural frequency, ϕ is an arbitrary phase angle determined by the initial conditions, and $n = 0, 1, 2, \ldots, \infty$. By substituting equations (2) into the three partial differential equations of motion for the body, expressed in cylindrical co-ordinates, one may verify that these are proper assumed forms for the displacements, and that θ and t are thereby uncoupled from ξ and ζ.

TABLE 2

Convergence of frequencies in $\omega R\sqrt{(\rho/G)}$ for the five lowest ζ-antisymmetric modes with $n = 1$, where $H/D = 0{\cdot}2$ and $\nu = 0{\cdot}3$

I	J	D	1	2	3	4	5
1	1	12	3·17854	8·21752	8·49207	11·20912	28·32614
3	1	24	2·79903	6·30186	8·17139	8·37331	9·92055
5	1	36	2·78186	5·87503	8·06383	8·30631	9·31771
7	1	48	2·78178	5·86208	8·05648	8·30325	9·21586
9	1	60	2·78177	5·86200	8·05623	8·30318	9·21243
10	1	66	2·78177	5·86200	8·05623	8·30318	9·21238
1	2	18	3·17654	8·21199	8·48836	11·15477	17·41577
3	2	36	2·79617	6·28169	8·15761	8·36294	9·86546
5	2	54	2·77967	5·85660	8·04636	8·29985	9·27091
7	2	72	2·77961	5·84440	8·03788	8·29662	9·17229
9	2	90	2·77961	5·84432	8·03772	8·29655	9·16873
1	3	24	3·17654	8·21199	8·48836	11·15456	16·95908
3	3	48	2·79613	6·27917	8·15719	8·36253	9·86451
5	3	72	2·77967	5·85651	8·04620	8·29980	9·27008
7	3	96	2·77961	5·84436	8·03778	8·29659	9·17212
9	3	120	**2·77960**	**5·84428**	**8·03762**	**8·29652**	**9·16856**
1	4	30	3·17654	8·21199	8·48836	11·15456	16·95127
3	4	60	2·79614	6·27971	8·15726	8·36259	9·86460
5	4	90	2·77967	5·85621	8·04612	8·29979	9·26966
7	4	120	2·77961	5·84436	8·03778	8·29659	9·17212
8	4	135	2·77960	5·84429	8·03772	8·29655	9·16903
1	5	36	3·17654	8·21199	8·48836	11·15456	16·95123
3	5	72	2·79613	6·27914	8·15718	8·36252	9·86450
5	5	108	2·77967	5·85650	8·04620	8·29980	9·27003
7	5	144	2·77961	5·84436	8·03778	8·29659	9·17212
1	6	42	3·17654	8·21199	8·48836	11·15456	16·95123
3	6	84	2·79616	6·28170	8·15748	8·36278	9·86484
5	6	126	2·77967	5·85651	8·04620	8·29980	9·27004
6	6	147	2·77962	5·84493	8·04512	8·29887	9·19670

TABLE 3

Comparison of non-dimensional frequencies $\omega R\sqrt{(\rho/G)}$ for antisymmetric modes with various ratios of thickness-to-diameter, from 3-D and 2-D Mindlin theory

			H/D							
n	s			0·05		0·075		0·1		0·125
0	1	3-D	**2**	0·4329	**2**	0·6381	**2**	0·8314	**2**	1·011
		2-D	**2**	0·4327	**2**	0·6375	**2**	0·8300	**2**	1·008
		(%)		(0·0)		(−0·1)		(−0·2)		(−0·2)
	2	3-D	**8**	1·763	**8**	2·477	**8**	3·059	**8**	3·524
		2-D	**8**	1·759	**8**	2·465	**8**	3·036	**8**	3·489
		(%)		(−0·3)		(−0·5)		(−0·7)		(−1·0)
	3	3-D		3·761		5·012		5·898		6·521
		2-D		3·741		4·964		5·821		6·415
		(%)		(−0·5)		(−0·9)		(−1·3)		(−1·6)
	4	3-D		6·214		7·895		8·948		9·582
		2-D		6·162		7·787		8·789		9·385
		(%)		(−0·8)		(−1·4)		(−1·8)		(−2·1)
1	1	3-D	**4**	0·9631	**4**	1·388	**4**	1·762	**4**	2·084
		2-D	**4**	0·9618	**4**	1·385	**4**	1·754	**4**	2·071
		(%)		(−0·1)		(−0·3)		(−0·4)		(−0·6)
	2	3-D		2·658		3·637		4·381		4·938
		2-D		2·6747		3·611		4·336		4·873
		(%)		(−0·4)		(−0·7)		(−1·0)		(−1·3)
	3	3-D		4·910		6·386		7·369		8·013
		2-D		4·876		6·312		7·254		7·864
		(%)		(−0·7)		(−1·2)		(−1·6)		(−1·9)
	4	3-D		7·532		9·379		10·463		11·014
		2-D		7·453		9·226		10·250		10·773
		(%)		(−1·0)		(−1·6)		(−2·0)		(−2·2)
2	1	3-D	**1**	0·2576	**1**	0·3812	**1**	0·4995	**1**	0·6118
		2-D	**1**	0·2575	**1**	0·3810	**1**	0·4991	**1**	0·6109
		(%)		(0·0)		(−0·1)		(−0·1)		(−0·1)
	2	3-D	**7**	1·616	**7**	2·275	**7**	2·817	**7**	3·253
		2-D	**7**	1·612	**7**	2·265	**7**	2·2798	**7**	3·224
		(%)		(−0·2)		(−0·5)		(−0·7)		(−0·9)
	3	3-D		3·623		4·839		5·706		6·316
		2-D		3·605		4·795		5·633		6·216
		(%)		(−0·5)		(−0·9)		(−1·3)		(−1·6)
	4	3-D		6·090		7·751		8·795		9·421
		2-D		6·039		7·646		8·640		9·228
		(%)		(−0·8)		(−1·3)		(−1·8)		(−2·0)
3	1	3-D	**3**	0·5891	**3**	0·8591	**3**	1·106	**3**	1·329
		2-D	**3**	0·5887	**3**	0·8580	**3**	1·104	**3**	1·326
		(%)		(−0·1)		(−0·1)		(−0·2)		(−0·3)
	2	3-D	**10**	2·361	**10**	3·249	**10**	3·936	**10**	4·458
		2-D	**10**	2·353	**10**	3·229	**10**	3·900	**10**	4·405
		(%)		(−0·3)		(−0·6)		(−0·9)		(−1·2)
	3	3-D		4·643		6·063		7·020		7·654
		2-D		4·613		5·997		6·915		7·516
		(%)		(−0·6)		(−1·1)		(−1·5)		(−1·8)
	4	3-D		7·293		9·105		10·179		10·742
		2-D		7·221		8·965		9·981		10·510
		(%)		(−1·0)		(−1·5)		(−1·9)		(−2·2)

Table 3—(*continued overleaf*)

TABLE 3—(*continued*)

n	s			H/D 0·05		0·075		0·1		0·125
4	1	3-D	**5**	1·016	**5**	1·458	**5**	1·843	**5**	2·172
		2-D	**5**	1·015	**5**	1·454	**5**	1·863	**5**	2·162
		(%)		(−0·1)		(−0·2)		(−0·3)		(−0·5)
	2	3-D		3·181		4·283		5·088		5·669
		2-D		3·166		4·248		5·030		5·589
		(%)		(−0·4)		(−0·8)		(−1·1)		(−1·4)
	3	3-D		5·702		7·298		8·318		8·950
		2-D		5·658		7·206		8·178		8·773
		(%)		(−0·8)		(−1·3)		(−1·7)		(−2·0)
	4	3-D		8·513		10·448		11·524		11·963
		2-D		8·415		10·266		11·278		11·767
		(%)		(−1·2)		(−1·8)		(−2·1)		(−1·6)
5	1	3-D	**6**	1·529	**6**	2·154	**6**	2·673	**6**	3·096
		2-D	**6**	1·526	**6**	2·147	**6**	2·660	**6**	3·077
		(%)		(−0·2)		(−0·3)		(−0·5)		(−0·6)
	2	3-D		4·059		5·355		6·255		6·875
		2-D		4·036		5·304		6·173		6·765
		(%)		(−0·6)		(−1·0)		(−1·3)		(−1·6)
	3	3-D		6·793		8·536		9·595		10·200
		2-D		6·731		8·414		9·419		9·986
		(%)		(−0·9)		(−1·4)		(−1·8)		(−2·1)
	4	3-D		9·743		11·776		12·823		13·062
		2-D		9·615		11·547		12·533		12·562
		(%)		(−1·3)		(−1·9)		(−2·3)		(−3·8)
6	1	3-D	**9**	2·116	**9**	2·929	**9**	3·570	**9**	4·072
		2-D	**9**	2·111	**9**	2·915	**9**	3·547	**9**	4·039
		(%)		(−0·3)		(−0·5)		(−0·6)		(−0·8)
	2	3-D		4·985		6·454		7·427		8·069
		2-D		4·952		6·382		7·317		7·927
		(%)		(−0·7)		(−1·1)		(−1·5)		(−1·8)
	3	3-D		7·907		9·773		10·850		11·403
		2-D		7·825		9·619		10·636		11·154
		(%)		(−1·0)		(−1·6)		(−2·0)		(−2·2)
	4	3-D		10·985		13·081		14·069		14·049
		2-D		10·819		12·810		13·741		13·780
		(%)		(−1·5)		(−2·1)		(−2·3)		(−1·9)

A complementary set of functions may also be used for equations (2), replacing $\cos n\theta$ by $\sin n\theta$, and conversely. This gives the same vibratory mode shapes rotated by 90° in θ, and the same frequencies, except for $n = 0$. For $n = 0$, equations (2) yield the axisymmetric modes which involve only u and w (for example, longitudinal and/or radial extension). However, the complementary set for $n = 0$ yields the torsional modes, which involve only v, uncoupled from u and w. Thus, for the circular or annular cross-section (but not for other cross-sections), there is no warping of the cross-section during torsional vibration.

Using algebraic polynomials which are mathematically complete, displacement functions U, V and W in equations (2) which are capable of satisfying any geometrical

TABLE 4

Comparison of frequencies $\omega R_o\sqrt{(\rho/G)}$ for the annular thick plates with $\nu = 0{\cdot}3$ by the 3-D Ritz (3DR), 3-D Hutchinson's series method (3DH), and Mindlin's 2-D plate theory (2DM)

$\frac{H}{D_o}$	$\frac{D_i}{D_o}$	n	Method	s			
				1	2	3	4
0·2	0·5		3DR	1·388	8·321	9·127	14·133
		0	3DH	1·398	8·327	9·128	10·398
			2DM	1·388	8·324	9·370	**10·593**
			3DR	1·943	8·039	8·534	8·945
		1	3DH	1·950	8·040	8·539	8·946
			2DM	1·951	8·189	8·659	9·162
			3DR	0·691	3·123	8·400	8·793
		2	3DH	6·901	3·127	8·404	8·794
			2DM	**6·923**	3·142	8·461	8·964
			3DR	1·680	4·450	8·808	8·986
		3	3DH	1·682	4·453	8·990	10·234
			2DM	1·684	4·475	8·899	9·076
0·5	0·5		3DR	1·984	5·772	8·258	9·084
		0	3DH	1·985	5·774	7·503	8·259
			2DM	1·985	6·720	7·547	10·010
			3DR	1·999	3·930	5·839	7·706
		1	3DH	2·000	3·930	5·841	6·401
			2DM	2·005	4·064	6·583	8·207
			3DR	1·039	2·846	5·172	6·157
		2	3DH	1·040	2·846	5·173	6·159
			2DM	1·040	2·860	5·399	6·730
			3DR	2·320	3·946	6·392	6·805
		3	3DH	2·321	3·946	6·392	6·806
			2DM	2·324	3·971	6·749	7·311

boundary conditions may be represented by

$$U(\xi,\zeta) = f_1(\xi)\sum_{i=0}^{I}\sum_{j=0}^{J} A_{ij}\xi^i\zeta^j$$

$$V(\xi,\zeta) = f_2(\xi)\sum_{k=0}^{K}\sum_{\ell=0}^{L} B_{k\ell}\xi^k\zeta^\ell$$

$$W(\xi,\zeta) = f_3(\xi)\sum_{m=0}^{M}\sum_{p=0}^{P} C_{mn}\xi^m\zeta^p \tag{3}$$

TABLE 5

Convergence of frequency $\omega R\sqrt{(\rho/G)}$ for the lowest antisymmetric mode of a circular plate with $\nu = 0{\cdot}344$ and $H/D = 0{\cdot}25$ based upon Hutchinson's series solution technique ($n = 1$)

	NZ			
NR	1	2	3	4
2	3·331	3·322	3·321	3·321
4	3·223	3·201	3·198	3·198
6	3·206	3·175	3·171	3·171
8	3·202	3·167	3·162	3·161
10	3·200	3·164	3·158	3·156
12	3·200	3·163	3·156	**3·154**

where f_i are all unity if no displacement constraints are imposed on any boundaries. If the outer edge is fixed and all other boundaries free,

$$f_1 = f_2 = f_3 = 1 - \xi. \tag{4}$$

If, as another example, both edges are fixed, then

$$f_1 = f_2 = f_3 = (1 - \xi)\left(\frac{R_i}{R_o} - \xi\right). \tag{5}$$

An additional plane of symmetry at $\zeta = 0$ exists for plates having both faces free. In such cases, one should take advantage of the symmetry by taking j and ℓ to be $0, 2, 4, \ldots$ and $p = 1, 3, 5, \ldots$ for the symmetric modes, and j and ℓ to be $1, 3, 5, \ldots$ and $p = 0, 2, 4, \ldots$ for the antisymmetric modes. For plate-like cylinders (for example, $H/D = 0{\cdot}5$ and less) the antisymmetric modes include the ones which are predominantly flexural, whereas the symmetric modes include those which are predominantly inplane stretching.

For the analysis of a circular plate with D and H only, considerable care must be exercised in choosing the lower limits of i, j, k, ℓ, m and p in equations (3). This is due to the necessity to avoid strain and stress singularities at $\xi = 0$. To circumvent this singularity, one must take: (1) For the axisymmetric modes ($n = 0$), $i = 1, 2, 3, \ldots, \infty$ and

TABLE 6

Convergence of frequency $\omega R\sqrt{(\rho/G)}$ for the same plate as in Table 5, based upon the Ritz method

	J			
I	1	2	3	4
1	3·5526	3·5446	3·5430	3·5430
3	3·1668	3·1601	3·1600	3·1600
5	3·1511	3·1458	3·1458	1·1458
7	3·1510	**3·1457**	3·1457	3·1457
9	3·1510	3·1457	3·1457	—

TABLE 7

Comparison of frequencies in $\omega R_o\sqrt{(\rho/G)}$ for the annular plate with $H/D_o = 0{\cdot}2941$, $D_i/D_o = 0{\cdot}1765$, and $\nu = 0{\cdot}3$ by the Ritz (3DR) method and the finite element method (3DF)

		s				
n	Method	1	2	3	4	5
For symmetric modes						
	3DR	3·0858	7·2372	7·8200	8·9145	9·5772
0	3DF	3·0874	7·2457	7·8345	8·9372	9·7051
	(%)	(0·05)	(0·12)	(0·18)	(0·26)	(1·39)
	3DR	2·7717	6·0272	6·9938	7·8951	
1	3DF	2·7778	6·0287	6·9986	7·9149	
	(%)	(0·22)	(0·03)	(0·07)	(0·25)	
	3DR	1·9684	4·0503	6·3799	7·7821	8·1282
2	3DF	1·9776	4·0535	6·3915	7·8033	8·1379
	(%)	(0·47)	(0·08)	(0·18)	(0·27)	(0·12)
For antisymmetric modes						
	3DR	1·7884	5·3168	6·7194	9·6715	
0	3DF	1·7899	5·3276	6·7422	9·7096	
	(%)	(0·09)	(0·20)	(0·34)	(0·39)	
	3DR	2·9046	5·5678	6·0365	6·1431	
1	3DF	2·9090	5·5755	6·0416	6·1547	
	(%)	(0·15)	(0·14)	(0·08)	(0·19)	
	3DR	1·1300	4·4052	6·1753	6·7662	7·6741
2	3DF	1·1324	4·4100	6·1907	6·7725	7·7279
	(%)	(0·21)	(0·11)	(0·25)	(0·09)	(0·70)

$m = 0, 1, 2, \ldots, \infty$. (2) For the torsional modes ($n = 0$), $k = 1, 2, 3, \ldots, \infty$. (3) For one other special case ($n = 1$), $i, k, m = 1, 2, 3, \ldots, \infty$ and terms $A_{00} + A_{01}\zeta$ and $B_{00} + B_{01}\zeta$ added to U and V, respectively. These are rigid body translation and rotation terms that are needed for the completeness of the admissible functions. (4) For general modes ($n \geqslant 2$), $i, k, m = 1, 2, 3, \ldots, \infty$.

The Ritz method uses the energy functionals for the vibrating system. The maximum potential energy during a vibratory cycle is due to the strain energy of deformation. It is

$$V_{\max} = \frac{G}{2} H \int_{-\frac{1}{2}}^{\frac{1}{2}} \int_A^1 \left\{ \frac{2\nu}{1-2\nu} \left(U_{,\xi} + \frac{n}{\xi} V + \frac{U}{\xi} + \frac{R_0}{H} W_{,\zeta} \right)^2 \Gamma_1 \right.$$
$$+ 2\left[(U_{,\xi})^2 + \left(\frac{n}{\xi} V + \frac{U}{\xi} \right)^2 + \left(\frac{R_o}{H} W_{,\zeta} \right)^2 \right] \Gamma_1$$
$$+ \left[\left(V_{,\xi} - \frac{n}{\xi} U - \frac{V}{\xi} \right)^2 + \left(\frac{R_o}{H} V_{,\zeta} - \frac{n}{\xi} W \right)^2 \right] \Gamma_2$$
$$\left. + \left(\frac{R_0}{H} U_{,\zeta} + W_{,\xi} \right)^2 \Gamma_1 \right\} \xi \, \mathrm{d}\xi \, \mathrm{d}\zeta \qquad (6)$$

where G is the shear modulus of elasticity, v is Poisson's ratio, subscripted symbols following commas denote differentiations, and the lower limit of integration A on ξ is R_i/R_0. For the circular plate, A becomes zero. In addition, Γ_1 and Γ_2 in equation (6) are defined by

$$\Gamma_1 = \int_0^{2\pi} \cos^2 n\theta \, \mathrm{d}\theta = \begin{cases} 2\pi, & \text{if } n = 0 \\ \pi, & \text{if } n > 0 \end{cases}$$

$$\Gamma_2 = \int_0^{2\pi} \sin^2 n\theta \, \mathrm{d}\,\theta = \begin{cases} 0, & \text{if } n = 0 \\ \pi, & \text{if } n > 0 \end{cases}. \tag{7}$$

The maximum kinetic energy during a vibratory cycle is

$$T_{\max} = \frac{\rho}{2}\omega^2 R_0^2 H \int_{-\frac{1}{2}}^{\frac{1}{2}} \int_A^1 (U^2\Gamma_1 + V^2\Gamma_2 + W^2\Gamma_1)\xi \, \mathrm{d}\xi \, \mathrm{d}\zeta \tag{8}$$

where ρ is mass per unit volume.

Free vibration frequencies are obtained by applying the minimizing conditions

$$\frac{\partial}{\partial A_{ij}}(V_{\max} - T_{\max}) = 0$$

$$\frac{\partial}{\partial B_{k\ell}}(V_{\max} - T_{\max}) = 0$$

$$\frac{\partial}{\partial C_{mp}}(V_{\max} - T_{\max}) = 0 \tag{9}$$

for all values of i, j, k, ℓ, m and p used in equations (3). This results in a generalized eigenvalue problem in the form of $\mathbf{Kx} = \lambda\mathbf{Mx}$, where $\mathbf{K}$ and $\mathbf{M}$ are stiffness and mass matrices, $\mathbf{x}$ is an eigenvector consisting of unknowns A_{ij}, $B_{k\ell}$, C_{mp} and λ is an eigenvalue expressed by the square of non-dimensional frequency or $\omega^2 R_o^2 \rho/G$. For a non-trivial solution the determinant of $(\mathbf{K} - \lambda\mathbf{M})$ is set equal to zero. From the zeros (eigenvalues) of this determinant, the non-dimensional frequency parameters are obtained. Corresponding mode shapes (eigenvectors) are determined by back-substitution of the eigenvalues, one-by-one, in the usual manner.

For hollow cylinders (i.e., annular plates), a local co-ordinate system is used, where θ and z are the same but a radial direction q measured from the middle of the cylindrical wall is introduced to the analysis (Figure 1). This local co-ordinate system has a great advantage in reducing early numerical instability or ill-conditioning [3]. In other words, relatively accurate frequencies can be obtained in comparison with those based upon cylindrical co-ordinates. The analysis based upon local co-ordinates (q, θ, z) follows the same procedure described above, but with different forms of energy functionals obtained

TABLE 8

3-D frequencies in $\omega R\sqrt{(\rho/G)}$ for symmetric modes of the circular plates with $\nu = 0{\cdot}3$, based upon the Ritz method

		H/D			
n	s	0·2	0·3	0·4	0·5
0^a	1	3·436	3·398	3·336	3·238
	2	8·589	7·468	5·740	4·643
	3	11·488	7·689	6·398	5·617
	4	11·610	9·245	7·397	6·381
	5	13·383	9·910	8·761	8·005
0^t	1	5·136	5·136	5·136	5·136
	2	8·417	8·417	7·854	6·283
	3	11·620	10·472	8·417	8·115
	4	14·796	11·620	9·384	8·417
	5	15·708	11·663	11·512	10·504
1	1	2·731	2·726	2·718	2·705
	2	5·864	5·665	5·233	4·595
	3	6·812	6·749	5·853	4·836
	4	9·903	7·737	6·700	6·439
	5	10·366	8·414	7·343	6·639
2	1	2·345	2·345	2·345	2·345
	2	4·230	4·204	4·143	3·966
	3	7·501	7·003	5·834	4·867
	4	8·560	7·733	6·263	5·623
	5	11·122	8·292	7·935	7·353
3	1	3·600	3·599	3·596	3·591
	2	5·793	5·693	5·303	4·612
	3	8·832	7·712	6·392	6·045
	4	10·105	8·165	7·058	6·498
	5	11·610	9·427	8·972	8·123
4	1	4·685	4·679	4·667	4·640
	2	7·349	6·961	5·931	5·230
	3	9·993	8·281	7·653	7·238
	4	11·262	8·871	7·939	7·681
	5	11·930	10·653	9·741	8·975
5	1	5·700	5·685	5·651	5·571
	2	8·834	7·726	6·549	6·034
	3	10·932	9·376	8·685	8·108
	4	11·987	9·664	9·243	9·177
	5	12·618	11·743	10·548	9·886
6	1	6·679	6·649	6·577	6·451
	2	10·166	8·308	7·288	6·950
	3	11·674	10·433	9·549	8·948
	4	12·571	10·799	10·701	10·614
	5	13·687	12·560	11·408	10·850

Table 8—(*continued overleaf*)

TABLE 8 (*continued*)

		H/D			
n	s	0·2	0·3	0·4	0·5
7	1	7·636	7·583	7·468	7·335
	2	11·173	8·937	8·126	7·902
	3	12·538	11·285	10·398	9·787
	4	13·229	12·179	12·097	11·679
	5	14·907	13·365	12·329	12·084
8	1	8·577	8·495	8·349	8·233
	2	11·846	9·645	9·022	8·860
	3	13·673	12·139	11·242	10·631
	4	13·942	13·528	13·187	12·560
	5	16·129	14·189	13·526	13·184
9	1	9·507	9·391	9·234	9·142
	2	12·418	10·425	9·945	9·818
	3	14·697	12·995	12·087	11·483
	4	14·906	14·820	14·133	13·392
	5	17·052	15·052	14·822	14·107

Note: 0^a = axisymmetric, 0^t = torsional.

same procedure described above, but with different forms of energy functionals obtained by a transformation of co-ordinates. Equations (6) and (8) are rewritten as

$$V_{\max} = \frac{G}{2} H \int_{-\frac{1}{2}}^{\frac{1}{2}} \int_{-\frac{1}{2}}^{\frac{1}{2}} \left\{ \frac{2v}{1-2v} \left(U_{,\xi} + \frac{n}{\gamma} V + \frac{U}{\gamma} + \frac{R_o - R_i}{H} W_{,\zeta} \right)^2 \Gamma_1 \right.$$

$$+ 2\left[(U_{,\xi})^2 + \left(\frac{n}{\gamma} V + \frac{U}{\gamma} \right)^2 + \left(\frac{R_o - R_i}{H} W_{,\zeta} \right)^2 \right] \Gamma_1$$

$$+ \left[\left(V_{,\xi} - \frac{n}{\gamma} U - \frac{V}{\gamma} \right)^2 + \left(\frac{R_o - R_i}{H} V_{,\zeta} - \frac{n}{\gamma} W \right)^2 \right] \Gamma_2$$

$$\left. + \left(\frac{R_o - R_i}{H} U_{,\zeta} + W_{,\xi} \right)^2 \Gamma_1 \right\} \gamma \, \mathrm{d}\xi \, \mathrm{d}\zeta \qquad (10)$$

$$T_{\max} = \frac{\rho}{2} \omega^2 (R_o - R_i)^2 H \int_{-\frac{1}{2}}^{\frac{1}{2}} \int_{-\frac{1}{2}}^{\frac{1}{2}} (U^2 \Gamma_1 + V^2 \Gamma_2 + W^2 \Gamma_1) \gamma \, \mathrm{d}\xi \, \mathrm{d}\zeta \qquad (11)$$

where ξ is redefined by $q/(R_o - R_i)$ and $\gamma = \xi + [(R_o + R_i)/(R_o - R_i)]/2$.

As it is well known, frequencies by the Ritz method converged in the manner of upper bounds to the exact values. These upper bounds are improved by increasing the numbers of polynomial terms in equaions (3). Since the algebraic polynomials of equations (3) form sets which are mathematically complete, as sufficient numbers of terms are taken, monotonic convergence to the exact frequencies is guaranteed.

TABLE 9

3-D frequencies in $\omega R\sqrt{(\rho/G)}$ for antisymmetric modes of the circular plates with $v = 0{\cdot}3$, based upon the Ritz method

		H/D			
n	s	0·2	0·3	0·4	0·5
0^a	1	1·464	1·896	2·193	2·402
	2	4·415	4·889	4·890	4·677
	3	7·353	6·847	6·359	6·145
	4	9·323	8·755	8·700	8·079
	5	11·088	10·182	9·066	8·221
0^t	1	7·854	5·236	3·927	3·142
	2	9·384	7·334	6·465	6·020
	3	11·512	9·913	9·288	8·984
	4	14·025	12·745	11·781	9·425
	5	16·751	15·695	12·265	10·733
1	1	2·780	3·249	3·314	3·088
	2	5·844	5·439	4·578	4·053
	3	8·038	5·867	4·892	4·595
	4	8·297	6·873	6·707	6·386
	5	9·169	8·220	7·641	7·278
2	1	0·9078	1·211	1·430	1·591
	2	4·089	4·475	4·330	4·040
	3	7·087	6·348	5·784	5·243
	4	8·881	6·773	5·936	5·850
	5	8·984	8·351	8·160	7·665
3	1	1·860	2·322	2·613	2·805
	2	5·353	5·572	5·270	4·962
	3	8·155	7·299	6·969	6·477
	4	9·723	7·918	7·128	6·994
	5	10·069	9·714	9·368	8·632
4	1	2·890	3·442	3·755	3·945
	2	6·561	6·564	6·172	5·870
	3	9·092	8·318	8·166	7·593
	4	10·715	9·140	8·286	8·062
	5	11·265	10·976	10·368	9·411
5	1	3·951	4·546	4·855	5·030
	2	7·709	7·492	7·067	6·779
	3	9·980	9·391	9·295	8·460
	4	11·814	10·361	9·383	9·148
	5	12·482	12·134	11·227	10·374
6	1	5·022	5·628	5·919	6·072
	2	8·795	8·393	7·965	7·692
	3	10·881	10·482	10·227	9·222
	4	12·961	11·542	10·489	10·183
	5	13·688	13·179	12·145	11·397

Table 9—(*continued overleaf*)

TABLE 9—(*continued*)

		H/D			
n	s	0·2	0·3	0·4	0·5
7	1	6·090	6·688	6·954	7·082
	2	9·825	9·287	8·870	8·609
	3	11·819	11·569	11·034	9·994
	4	14·125	12·646	11·556	11·134
	5	14·870	14·136	13·129	12·326
8	1	7·151	7·727	7·963	8·067
	2	10·805	10·181	9·781	9·528
	3	12·798	12·639	11·799	10·809
	4	15·287	13·640	12·576	12·027
	5	16·021	15·080	13·992	13·270
9	1	8·202	8·747	8·953	9·035
	2	11·750	11·080	10·697	10·449
	3	13·810	13·679	12·571	11·666
	4	16·441	14·527	13·552	12·887
	5	17·139	16·077	14·871	14·222

Note: 0^a = axisymmetric, 0^t = torsional.

3. CONVERGENCE STUDIES

To demonstrate the convergence of the method, numerical results are presented for a completely free, circular plate with $H/D = 0{\cdot}2$ and Poisson's ratio $\nu = 0{\cdot}3$. Equal numbers of polynomial terms were taken for U, V and W in equations (3) in either ξ-co-ordinate or ζ-co-ordinate (i.e., $I = K = M$ or $J = L = P$), although a computational optimization could be obtained for some configurations and some mode shapes by using unequal numbers of polynomial terms. For a typical circular plate, more polynomial terms in the ξ-co-ordinate are required than in ζ (i.e., $I > J$). Thus, the appropriate scheme for convergence study is to increase I from 1 until numerical ill-conditioning occurs, while keeping J at 1, 2, 3, and so on.

The non-dimensional frequencies ($\omega R\sqrt{(\rho/G)}$) are listed in Table 1 for the first five modes which are both axisymmetic ($n = 0$) and symmetric (in ζ). The first two columns show the upper limits of I ($= K = M$) and J ($= L = P$) used in equations (3). The third column indicates the size of the resulting eigenvalue determinant (D). As J increases, I decreases due to ill-conditioning. Bold-faced values in Table 1 indicate the lowest frequencies for the smallest determinant sizes from which they are obtained. First and second frequencies converged to six-digit accurate values of 3·43638 and 8·58867 with $(I, J) = (3, 2)$ and $(7, 3)$, respectively but the other frequencies are of three- or four-digit accuracy. The maximum size of determinant (D) is 98.

Table 2 shows frequencies for the first five antisymmetric (in ζ) modes having $n = 1$. Similar to Table 1, the lowest values are obtained from the data set with $J = 3$. First and second frequencies converged to five-digit accurate values, while the remaining ones are of only three- or four-digit accuracy. The maximum size of determinant (D) achieved is, however, increased to 147, mainly because all three displacement components are involved for modes other than $n = 0$.

All computations above were performed in double precision (16 significant figures). Higher precision (i.e., quadruple precision) computation would produce more accurate

Table 10

3-D frequencies in $\omega R\sqrt{(\rho/G)}$ for symmetric modes of the circular plates with $\nu = 0$, based upon the Ritz method

		H/D			
n	s	0·2	0·3	0·4	0·5
0^a	1	2·604	2·604	2·604	2·604
	2	7·540	6·502	4·835	3·871
	3	9·810	7·405	5·554	4·443
	4	10·874	7·429	6·102	5·518
	5	11·107	7·540	7·540	7·386
0^t	1	5·136	5·136	5·136	5·136
	2	8·417	8·417	7·854	6·283
	3	11·620	10·472	8·417	8·115
	4	14·796	11·620	9·384	8·417
	5	15·708	11·663	11·512	10·504
1	1	2·474	2·474	2·474	2·474
	2	5·003	5·003	4·986	4·017
	3	6·734	6·565	5·003	4·508
	4	9·590	6·734	5·458	5·003
	5	9·845	7·277	6·734	6·328
2	1	2·336	2·336	2·336	2·336
	2	3·796	3·796	3·796	3·796
	3	6·783	6·741	5·079	4·056
	4	8·301	6·783	5·819	5·164
	5	9·949	7·277	6·783	6·783
3	1	3·545	3·545	3·545	3·545
	2	5·257	5·257	5·249	4·366
	3	8·298	6·883	5·257	5·257
	4	9·895	7·618	6·490	5·952
	5	10·120	8·298	8·298	7·739
4	1	4·571	4·571	4·571	4·571
	2	6·775	6·775	5·618	4·919
	3	9·666	7·074	6·775	6·757
	4	10·320	8·201	7·261	6·775
	5	10·918	9·666	9·253	8·481
5	1	5·529	5·529	5·529	5·529
	2	8·297	7·393	6·159	5·631
	3	10·502	8·297	8·064	7·550
	4	10·956	8·901	8·297	8·297
	5	11·219	10·956	9·991	9·272
6	1	6·457	6·457	6·457	6·435
	2	9·808	7·842	6·827	6·457
	3	10·704	9·665	8·872	8·332
	4	11·688	9·808	9·808	9·808
	5	12·201	11·848	10·761	10·094

Table 10—(*continued overleaf*)

TABLE 10—(*continued*)

		H/D			
n	s	0·2	0·3	0·4	0·5
7	1	7·369	7·369	7·369	7·294
	2	10·973	8·401	7·580	7·369
	3	11·304	10·462	9·673	9·107
	4	12·265	11·304	11·304	10·932
	5	13·423	12·611	11·567	11·304
8	1	8·272	8·272	8·272	8·181
	2	11·322	9·047	8·390	8·272
	3	12·780	11·274	10·465	9·882
	4	12·917	12·780	12·402	11·772
	5	14·635	13·379	12·780	12·780
9	1	9·169	9·169	9·169	9·086
	2	11·750	9·760	9·237	9·169
	3	13·623	12·091	11·252	10·662
	4	14·232	14·163	13·258	12·611
	5	15·846	14·232	14·232	13·811

Note: 0^a = axisymmetric, 0^t = torsional.

frequencies. There are some other ways to avoid the early ill-conditioning seen in the tables, such as using orthogonal polynomials.

Extensive convergence studies for the 3-D Ritz method have also been made in reference [5] for hollow cylinders (for which the annular, thick plate is a special case). Convergence rates were observed which are similar to those exhibited for solid plates in Tables 1 and 2.

4. COMPARISON WITH MINDLIN'S THEORY

The vibrations of thick plates have received much attention in a series of papers by Mindlin and his co-workers. Mindlin and Deresiewicz used Mindlin's plate theory to consider axisymmetric ($n = 0$) vibration of circular plates in reference [11] and to consider the ($n = 1$) mode in reference [12]. Irie *et al*. [13] obtained frequency data for circular plates with various boundary conditions, including a free edge. The thickness ratios taken in their paper are 0·025, 0·05, 0·075, 0·1 and 0·125 with a Poisson's ratio (ν) of 0·3.

Table 3 shows the comparison of dimensionless frequencies ($\omega R\sqrt{(\rho/G)}$) from the 3-D and Mindlin's theories for circular plates of $H/D = 0{\cdot}05$, 0·075, 0·1 and 0·125. A total of 28 modes—seven circumferential wave numbers (i.e., $n = 0, 1, 2, \ldots, 6$) and four radial mode numbers (i.e., $s = 1, 2, 3, 4$)—are selected for the frequency comparison. The bold-faced integers in front of frequency data indicate the ascending order of the ten lowest frequencies. In addition, the numbers in the parentheses are the percentage differences expressed by

$$\text{Difference (\%)} = \frac{\text{(2-D frequency)} - \text{(3-D frequency)}}{\text{3-D frequency}}. \tag{12}$$

From the table, it is seen that the lowest ten frequencies arise in the order of $(n, s) = (2, 1), (0, 1), (3, 1), (1, 1), (4, 1), (5, 1), (2, 2), (0, 2), (6, 1)$ and $(3, 2)$, regardless of

TABLE 11

3-D frequencies in $\omega R\sqrt{(\rho/G)}$ for antisymmetric modes of the circular plates with $\nu = 0$, based upon the Ritz method

		H/D			
n	s	0·2	0·3	0·4	0·5
0[a]	1	1·148	1·503	1·749	1·922
	2	3·839	4·324	4·403	4·283
	3	6·664	6·490	6·020	5·698
	4	8·896	8·129	7·969	7·329
	5	10·331	9·589	8·534	7·989
0[t]	1	7·854	5·236	3·927	3·142
	2	9·384	7·334	6·465	6·020
	3	11·512	9·913	9·288	8·984
	4	14·025	12·745	11·781	9·425
	5	16·751	15·695	12·265	10·733
1	1	2·355	2·797	2·934	2·854
	2	5·206	5·253	4·443	3·852
	3	7·755	5·715	4·763	4·389
	4	8·172	6·450	6·176	5·961
	5	8·716	7·836	7·220	6·629
2	1	0·8857	1·189	1·411	1·575
	2	3·588	4·003	3·981	3·789
	3	6·447	6·108	5·589	5·030
	4	8·589	6·614	5·659	5·477
	5	8·861	7·759	7·627	7·278
3	1	1·801	2·272	2·574	2·776
	2	4·791	5·085	4·895	4·644
	3	7·547	6·968	6·667	6·273
	4	9·405	7·724	6·812	6·493
	5	9·806	9·037	8·872	8·025
4	1	2·793	3·369	3·703	3·909
	2	5·950	6·054	5·742	5·470
	3	8·512	7·894	7·696	7·330
	4	10·333	8·921	8·042	7·578
	5	10·887	10·246	9·723	8·781
5	1	3·822	4·457	4·796	4·990
	2	7·056	6·945	6·567	6·292
	3	9·394	8·875	8·681	8·139
	4	11·372	10·143	9·241	8·736
	5	12·025	11·365	10·523	9·700
6	1	4·866	5·529	5·857	6·030
	2	8·107	7·793	7·387	7·116
	3	10·257	9·880	9·605	8·918
	4	12·469	11·355	10·332	9·737
	5	13·186	12·382	11·435	10·829

Table 11—(*continued overleaf*)

Table 11—(*continued*)

n	s	H/D 0·2	0·3	0·4	0·5
7	1	5·913	6·583	6·890	7·037
	2	9·100	8·622	8·208	7·946
	3	11·140	10·884	10·474	9·717
	4	13·587	12·507	11·287	10·625
	5	14·351	13·330	12·448	11·740
8	1	6·957	7·619	7·899	8·020
	2	10·041	9·444	9·034	8·782
	3	12·057	11·874	11·309	10·545
	4	14·704	13·527	12·171	11·469
	5	15·507	14·298	13·346	12·572
9	1	7·996	8·638	8·887	8·984
	2	10·938	10·265	9·865	9·625
	3	13·005	12·843	12·134	11·397
	4	15·808	14·399	13·036	12·296
	5	16·640	15·299	14·167	13·415

Note: 0^a = axisymmetric, 0^t = torsional.

the theories used. A similar trend is found to exist with the lowest frequencies of thin circular plates [14]. Because the thickness ratio of 0·125 is not very large, it is not surprising that Mindlin's theory gives reasonably accurate frequencies compared to the 3-D results, at least for the lower wave numbers. For instance, the percentage differences of the lowest ten frequencies are at most within $-1{\cdot}2\%$ for the case of $H/D = 0{\cdot}125$, and this occurs for the tenth frequency. The largest difference in the table is only $-3{\cdot}8\%$ and occurs for the (5, 4) mode. The (5, 4) mode shape has five nodal diameters and three interior nodal circles (lines of zero w-displacement). For such a mode the wave lengths are much shorter than those of the first ten frequencies. The negative sign in the percentage differences indicates that Mindlin's plate theory produces underestimated frequencies. That is, while it provides improved 2-D results, compared with thin plate theory, it overcorrects them.

Table 4 shows a comparison of frequencies $\omega R_o\sqrt{(\rho/G)}$ from 3-D and the Mindlin solutions for annular plates of $(H/D_o, D_i/D_o) = (0{\cdot}2, 0{\cdot}5)$ and $(0{\cdot}5, 0{\cdot}5)$ with $\nu = 0{\cdot}3$. The Mindlin data were taken from Hutchinson's paper [7]. Although for most frequencies, good agreement between them is observed, some serious diagreements are also seen. For the annular plate with $(H/D_o, D_i/D_o) = (0{\cdot}2, 0{\cdot}5)$, the fourth axisymmetric frequency of $(n, s) = (0, 4)$ is 10·593 and the frequency of $(n, s) = (2, 1)$ is 6·923. The corresponding 3-D frequencies are 14·133 and 0·691. Clearly, 6·923 is a typographical error, which should be read to be 0·6923 because it is higher than that (3·142) of the next mode, i.e., $(n, s) = (2, 2)$.

5. COMPARISON WITH OTHER 3-D SOLUTIONS

Many researchers investigated the problem of 3-D vibrating bodies such as disks. Among them, Hutchinson [6] presented the 3-D analytical solutions for the vibrations of thick, free, solid circular plates. His solutions are based upon series consisting of Bessel functions of the first kind in r and trigonometric functions in θ and z, each of which satisfies term by term the governing equations of 3-D elasticity and some boundary conditions on

TABLE 12

3-D frequencies in $\omega R\sqrt{(\rho/G)}$ for symmetric modes of the circular plates with $\nu = 0{\cdot}499$, based upon the Ritz method

n	s	H/D 0·2	0·3	0·4	0·5
0^a	1	4·163	3·973	3·730	3·459
	2	8·954	7·469	6·293	5·279
	3	11·564	8·679	6·871	6·151
	4	12·927	9·739	8·602	7·791
	5	13·848	11·586	10·269	9·680
0^t	1	5·136	5·136	5·136	5·136
	2	8·417	8·417	7·854	6·283
	3	11·620	10·472	8·417	8·115
	4	14·796	11·620	9·384	8·417
	5	15·708	11·663	11·512	10·504
1	1	2·849	2·838	2·821	2·792
	2	6·381	5·904	5·249	4·653
	3	6·983	6·755	6·377	5·279
	4	9·921	8·305	6·826	6·614
	5	10·410	8·923	7·617	6·815
2	1	2·349	2·349	2·348	2·348
	2	4·422	4·366	4·246	3·996
	3	7·770	7·020	6·064	5·307
	4	8·756	8·043	6·674	5·868
	5	11·153	8·748	8·131	7·493
3	1	3·619	3·616	3·612	3·604
	2	6·011	5·816	5·323	4·676
	3	8·989	7·840	6·899	6·483
	4	10·148	8·691	7·372	6·770
	5	11·996	9·764	9·149	8·309
4	1	4·724	4·713	4·693	4·652
	2	7·545	6·986	6·014	5·354
	3	10·051	8·682	8·128	7·516
	4	11·311	9·321	8·256	8·071
	5	12·614	11·013	9·964	9·225
5	1	5·758	5·731	5·676	5·574
	2	8·970	7·785	6·699	6·206
	3	10·949	9·814	9·048	8·383
	4	12·300	10·086	9·603	9·511
	5	13·307	12·037	10·821	10·207
6	1	6·753	6·699	6·593	6·454
	2	10·215	8·451	7·495	7·159
	3	11·784	10·909	9·910	9·239
	4	13·080	11·108	10·990	10·868
	5	14·325	12·875	11·734	11·234

Table 12—(*continued overleaf*)

TABLE 12—(*continued*)

		H/D			
n	s	0·2	0·3	0·4	0·5
7	1	7·722	7·631	7·478	7·341
	2	11·192	9·149	8·379	8·142
	3	12·732	11·763	10·768	10·100
	4	13·795	12·414	12·321	12·009
	5	15·540	13·709	12·700	12·323
8	1	8·672	8·536	8·359	8·243
	2	11·940	9·916	9·311	9·131
	3	13·841	12·628	11·627	10·970
	4	14·540	13·697	13·537	12·900
	5	16·743	14·567	13·758	13·359
9	1	9·606	9·426	9·247	9·157
	2	12·602	10·745	10·266	10·120
	3	15·015	13·495	12·490	11·850
	4	15·329	14·947	14·583	13·694
	5	17·639	15·458	14·949	14·357

Note: 0^a = axisymmetric, 0^t = torsional.

shear stress. Other boundary conditions have to be satisfied approximately by imposing orthogonalizing conditions on them.

Most of his results presented were plotted as frequency versus height-to-diameter ratios with $\nu = 0{\cdot}344$. However, there were some data in the form of tables for convergence studies, and some of them are selected for comparison with the present 3-D solutions. Table 5 shows the convergence of dimensionless frequency ($\omega R\sqrt{(\rho/G)}$) for the lowest antisymmetric mode with $n = 1$ in the case of $H/D = 0{\cdot}25$. NR and NZ in the table represent the number of terms Hutchinson used in radial and axial directions, respectively. Even though the lowest frequency obtained was 3·154 (bold-faced), it may not be a converged one. Thus it seems that Hutchinson's series solutions converge somewhat slowly.

Table 6, on the contrary, shows how well and rapidly the frequencies converge when using the Ritz method. For the same parameters as in Table 5, it gives a lowest frequency of 3·1457 which is exact to five digits. This frequency is attained with $I = 7$ and $J = 2$, where I and J are the upper limits of the polynomial terms used in equations (3). By looking at the frequencies with $I = 7$, $J = 3$ and $I = 9$, $J = 2$, one finds that it has converged at that value.

Hutchinson [7] also used the series method to obtain 3-D solutions for annular plates. Some of his results are seen in Table 4. It is seen there that most of his results agree well with those from the present 3-D Ritz method. The disagreements are mainly due to a lack of complete convergence in his values. However, there are other disagreements in Table 4 which are larger. These larger disagreements are: (1) For $H/D_o = 0{\cdot}2$, $(n, s) = (0, 4)$. The value of 10·398 presented by Hutchinson is actually for the second antisymmetric torsion mode (see Table 15 at the end of the present work). Table 4 is intended only to show flexural (coupled with thickness-shear) deformation modes, which the Mindlin theory can deal with. (2) For $H/D_o = 0{\cdot}2$, $(n, s) = (2, 1)$. The 3-D Hutchinson frequency of 6·901 is clearly a typographical error. It should be 0·6901. (3) For $H/D_o = 0{\cdot}2$, $(n, s) = (3, 4)$. The

Table 13

3-D frequencies in $\omega R\sqrt{(\rho/G)}$ for antisymmetric modes of the circular plates with $\nu = 0{\cdot}499$, based upon the Rtiz method

		H/D			
n	s	0·2	0·3	0·4	0·5
0^a	1	1·754	2·235	2·551	2·767
	2	4·908	5·337	5·272	4·978
	3	7·872	7·110	6·583	6·406
	4	9·635	9·174	9·085	8·201
	5	11·688	10·551	9·311	8·702
0^t	1	7·854	5·236	3·927	3·142
	2	9·384	7·334	6·465	6·020
	3	11·512	9·913	9·288	8·984
	4	14·025	12·745	11·781	9·425
	5	16·751	15·695	12·265	10·733
1	1	3·162	3·601	3·534	3·185
	2	6·335	5·522	4·706	4·173
	3	8·144	5·943	4·971	4·775
	4	8·361	7·282	7·094	6·616
	5	9·659	8·392	7·786	7·441
2	1	0·9200	1·222	1·440	1·599
	2	4·515	4·790	4·499	4·140
	3	7·502	6·490	5·887	5·354
	4	9·008	6·863	6·146	6·093
	5	9·148	8·796	8·423	7·739
3	1	1·892	2·347	2·631	2·818
	2	5·798	5·855	5·437	5·088
	3	8·493	7·495	7·081	6·572
	4	9·853	8·031	7·383	7·286
	5	10·268	10·152	9·490	8·636
4	1	2·940	3·475	3·776	3·959
	2	7·013	6·831	6·357	6·027
	3	9·394	8·566	8·297	7·661
	4	10·868	9·260	8·547	8·396
	5	11·634	11·363	10·405	9·506
5	1	4·015	4·583	4·877	5·044
	2	8·159	7·760	7·276	6·970
	3	10·284	9·684	9·439	8·534
	4	11·978	10·470	9·644	9·490
	5	12·891	12·426	11·277	10·506
6	1	5·095	5·667	5·941	6·086
	2	9·239	8·673	8·203	7·918
	3	11·209	10·818	10·372	9·305
	4	13·126	11·628	10·766	10·537
	5	14·122	13·373	12·222	11·565

Table 13—(*continued overleaf*)

TABLE 13—(*continued*)

n	s	H/D 0·2	0·3	0·4	0·5
7	1	6·169	6·727	6·975	7·096
	2	10·262	9·586	9·138	8·871
	3	12·182	11·947	11·167	10·079
	4	14·282	12·705	11·881	11·505
	5	15·324	14·264	13·255	12·572
8	1	7·232	7·764	7·984	8·083
	2	11·239	10·503	10·080	9·826
	3	13·199	13·059	11·926	10·891
	4	15·431	13·676	12·952	12·408
	5	16·499	15·178	14·258	13·586
9	1	8·283	8·783	8·974	9·052
	2	12·187	11·428	11·029	10·784
	3	14·245	14·137	12·695	11·745
	4	16·568	14·560	13·974	13·279
	5	17·648	16·158	15·179	14·607

Note: 0^a = axisymmetric, 0^t = torsional.

3-D Hutchinson value of 10·234 is actually for $s = 5$ (see Table 15, where 10·2331 is listed for this mode). (4) For $H/D_o = 0{\cdot}5$, $(n, s) = (0, 3)$, $(0, 4)$ and $(1, 4)$. The 3-D Hutchinson frequencies of 7·503, 8·259 and 6·401, respectively, for these modes are much lower than the converged Ritz values shown. Because 8·259 is close to the Ritz value of 8·258, it may be that 7·503 is an extraneous root.

Gladwell and Vijay [15] used the finite element to obtain natural frequencies of annular plates for modes up to $n = 2$, using toroidal elements. In Table 7, frequencies from the Ritz and finite element methods are compared for the annular plate having $(H/D_o, D_i/D_o) = (0{\cdot}2941, 0{\cdot}1765)$ with $\nu = 0{\cdot}3$. From the table, it is seen that none of the frequencies from the finite element method are lower than those from the Ritz method. The finite element results are quite accurate since most frequencies have differences of less than 1·0%. The largest difference is at most 1·39% for the mode $(n, s) = (0, 5)$.

6. ACCURATE NATURAL FREQUENCIES OF CIRCULAR AND ANNULAR PLATES

Having had its convergence and accuracy established, the 3-D Rtiz method is now used to obtain accurate frequencies for completely free circular and annular plates.

In Tables 8 and 9, non-dimensional frequencies $\omega R\sqrt{(\rho/G)}$ are presented for circular plates with $H/D = 0{\cdot}2, 0{\cdot}3, 0{\cdot}4, 0{\cdot}5$ and $\nu = 0{\cdot}3$, for modes which are symmetric and antisymmetric, respectively, to the midplane of the plate. There are 55 frequencies from $(n, s) = (0, 1)$ to $(9, 5)$. The symmetric modes involve midplane stretching (except for the torsional modes), whereas the antisymmetric modes include those which are predominantly flexural (as well as thickness-shear modes). Rigid body mode frequencies, which are zero, are excluded from the tables. Hutchinson [6] gave 10 plots of $\omega R\sqrt{(\rho/G)}$ versus H/D, with $n = 0$–4, including the symmetric and antisymmetric modes. The range of H/D was between 0 and 2, and the frequency parameter was displayed within 0–5. There are good agreements between the results of Tables 8 and 9 and their plots except for two plots for

TABLE 14

3-D frequencies in $\omega R_o \sqrt{(\rho/G)}$ for symmetric modes of the annular plates with $H/D_o = 0{\cdot}2$ and $\nu = 0{\cdot}3$, based upon the Ritz method

		D_i/D_0		
n	s	0·1	0·5	0·9
0^a	1	3·319	2·234	1·698
	2	8·161	9·957	5·905
	3	11·353	11·343	13·222
	4	11·548	12·207	20·258
	5	13·024	14·295	33·271
0^t	1	5·142	6·814	15·708
	2	8·457	12·856	31·416
	3	11·739	15·708	31·482
	4	15·044	17·122	35·183
	5	15·708	19·046	44·476
1	1	2·748	2·806	2·393
	2	6·031	7·372	5·953
	3	6·879	9·868	13·119
	4	10·233	11·386	15·906
	5	10·453	12·077	20·279
2	1	2·210	0·9490	0·1382
	2	4·149	4·177	3·771
	3	6·839	8·630	6·097
	4	8·493	9·721	12·897
	5	10·460	11·516	16·416
3	1	3·594	2·249	0·3883
	2	5·788	5·717	5·306
	3	8·733	9·441	6·330
	4	10·079	10·270	12·686
	5	11·545	11·744	17·112
4	1	4·685	3·622	0·7372
	2	7·349	7·209	6·634
	3	9·988	9·626	6·875
	4	11·260	11·310	12·574
	5	11·926	12·130	17·919
5	1	5·700	4·969	1·177
	2	8·834	8·575	7·029
	3	10·932	10·028	8·375
	4	11·987	11·924	12·629
	5	12·617	12·671	18·801
6	1	6·679	6·237	1·699
	2	10·166	9·806	7·483
	3	11·674	10·630	9·732
	4	12·571	12·467	12·952
	5	13·687	13·349	19·732

Note: 0^a = axisymmetric, 0^t = torsional.

TABLE 15

3-D frequencies in $\omega R_o\sqrt{(\rho/G)}$ for antisymmetric modes of the annular platers with $H/D_o = 0{\cdot}2$ and $\nu = 0{\cdot}3$, based upon the Ritz method

		D_i/D_o		
n	s	0·1	0·5	0·9
0^a	1	1·433	1·388	1·648
	2	4·491	8·321	12·694
	3	7·432	9·127	25·935
	4	9·620	14·133	27·155
	5	10·874	15·812	33·814
0^t	1	7·854	7·854	7·854
	2	9·388	10·398	23·562
	3	11·542	15·065	32·447
	4	14·124	20·602	39·270
	5	16·971	23·562	39·323
1	1	2·717	1·943	1·688
	2	5·643	8·039	8·084
	3	7·619	8·534	12·726
	4	8·238	8·945	23·512
	5	9·325	10·876	26·046
2	1	0·8909	0·6907	0·2769
	2	4·064	3·123	1·915
	3	7·018	8·400	8·707
	4	8·782	8·793	12·822
	5	8·969	9·233	23·391
3	1	1·859	1·681	0·8203
	2	5·351	4·450	2·382
	3	8·144	8·808	9·598
	4	9·719	8·986	12·982
	5	10·064	10·233	23·254
4	1	2·890	2·771	1·479
	2	6·561	5·805	3·036
	3	9·091	9·238	10·651
	4	10·715	9·587	13·202
	5	11·264	11·357	23·145
5	1	3·951	3·881	2·163
	2	7·709	7·141	3·832
	3	9·980	9·857	11·797
	4	11·814	10·394	13·483
	5	12·482	12·520	23·091
6	1	5·022	4·984	2·852
	2	8·795	8·421	4·728
	3	10·881	10·641	12·988
	4	12·961	11·372	13·827
	5	13·689	13·686	23·111

Note: 0^a = axisymmetric, 0^t = torsional.

$n = 4$. These two plots are so unusual that no reasonable explanation can be made. Indeed, he recently revised his paper to correct an error in the plots shown for the circumferential order four [16]. The new plotted frequencies are found to be somewhat higher than those in the tables, which indicates that his plots may be based upon inadequately converged frequencies.

It is interesting to note that some of the torsional mode ($n = 0$) frequencies in Table 8 (5·136, 8·417, 11·620) are independent of H/D. These are for modes which have cylindrical nodal *surfaces* along through the thickness of the plate. On the other hand, frequencies which are proper multiples of π (15·708, 10·472, 7·854, 6·283) are for modes which have circular cross-sections as nodal planes.

To show the influence of Poisson's ratio on the frequencies, Tables 10 to 13 are also presented. Tables 10 and 11 display the frequencies of symmetric and antisymmetric modes for the thickness ratios of Tables 8 and 9, except with $v = 0$, and Tables 12 and 13 are for $v = 0{\cdot}499$. (The upper limit of $v = 0{\cdot}5$ for an isotropic material cannot be achieved exactly with the existing computer program due to a singularity.) It is seen that the torsional frequencies do not depend upon Poisson's ratio.

Finally, Tables 14 and 15 give the frequencies $\omega R_o\sqrt{(\rho/G)}$ for the annular plates with $(H/D_o, D_i/D_o) = (0{\cdot}2, 0{\cdot}1), (0{\cdot}2, 0{\cdot}5)$ and $(0{\cdot}2, 0{\cdot}9)$ with $v = 0{\cdot}3$. There are eight sets of circumferential modes ranging from 0 to 6. It is noted that the lowest symmetric and antisymmetric modes come from $(n, s) = (2, 1)$, regardless of D_i/D_o. However, the frequencies are quite different, i.e., 2·2099 (S) and 0·8909 (A) for $D_iD_o = 0{\cdot}1$, 0·9490 (S) and 0·6907 (A) for $D_iD_o = 0{\cdot}5$, and 0·1382 (S) and 0·2769 (A) for $D_i/D_o = 0{\cdot}9$, where (S) and (A) mean symmetric and antisymmetric frequencies, respectively. Thus, it is observed that the fundamental mode shifts from antisymmetric (2, 1) to symmetric (2, 1) as the annular plate becomes a ring type of geometry. This is because the out-of-plane, flexural modes of plate-like configurations have lower frequencies than the in-plane, stretching modes. This is seen for all circumferential modes (n). Note that Table 15 contains some of the 3-D frequencies obtained by the Ritz method shown in Table 4.

7. CONCLUDING REMARKS

Extensive and accurate frequency data determined by the 3-D Ritz analysis have been presented for circular and annular plates. The analysis uses the 3-D equations of the theory of elasticity in their general forms for isotropic materials. They are only limited to small strains. No other constraints are placed upon the displacements. This is in stark contrast with the 2-D plate theories, which make very limiting assumptions about the displacement variations through the plate thickness.

Thorough convergence studies of the type shown in Tables 1 and 2 have been made [5] which indicate that the benchmark frequency values given in Tables 8–15 have converged to at least four significant figures. Because the admissible functions given by equations (3) are mathematically complete, they are capable of representing any deformation of the plate. That is, there are no constraints on the displacements. Thus, as sufficient polynomial terms are taken in equations (3), the frequencies will converge to the exact values, and the frequencies in Tables 8–15 may be considered as being exact to four digits.

The high accuracy is obtained with reasonable computational time because, although the analysis is 3-D, one variable (θ) is separated out early in equations (2), due to the required periodicity of the displacements in θ (i.e., $f(\theta + 2\pi) = f(\theta)$). This reduces the problem to a sequence of 2-D mathematical problems, one for each circumferential wave number, n. The 2-D problems require much less computer time and capacity than would a 3-D problem.

The extensive data includes frequencies for all vibration modes which are symmetric with respect to the midplane ($\zeta = 0$) of the plate, as well as those which are antisymmetric. The symmetric modes involve midplane stretching ($u \neq 0, v \neq 0$), except for the case $n = 0$, which is torsional. The antisymmetric modes are combinations of predominantly bending and thickness-shear deformations (except for the torsional modes). For the thinner plates the antisymmetric modes are typically the most important. For example, Tables 8 and 9 show that for $H/D = 0{\cdot}2$, the first two frequencies, and seven of the first ten, are associated with antisymmetric modes; but, for $H/D = 0{\cdot}5$, only half of the first ten frequencies are for antisymmetric modes.

The frequencies given in Tables 8–15 serve as valuable benchmark results against which results from 2-D thick plate theories or approximate methods (for example, finite elements, finite differences) may be compared in order to establish their accuracies. Besides the 2-D Mindlin theory used here for comparison (Tables 3 and 4), there are higher order 2-D plate theories proposed by numerous authors. Their governing equations are much more complicated than those of the Mindlin theory. One wonders how accurate their frequencies would be in representing a 3-D problem.

The 3-D method of analysis has been presented in a form which admits fixed boundaries as well as free ones, and it could be applied straightforwardly to such problems. Thus, one could obtain accurate frequencies for "clamped" circular plates, or for annular plates having one or both circular boundaries "clampled". The "clamping" simply requires all three displacement components at a boundary to be zero. Nothing is said about their slopes. One would expect the convergence of such solutions to be slower than that for a free boundary because of the stress singularities which arise at the top and bottom corners ($\zeta = \pm\frac{1}{2}$) of the fixed boundaries.

REFERENCES

1. A. W. LEISSA and J. SO 1995 *Journal of the Acoustical Society of America* **98**, 2122–2135. Comparisons of vibration frequencies for rods and beams from one-dimensional and three-dimensional analyses.
2. A. W. LEISSA and J. SO 1995 *Journal of the Acoustical Society of America* **98**, 2136–2141. Accurate vibration frequencies of circular cylinders from three-dimensional analysis.
3. J. SO and A. W. LEISSA *Journal of Vibration and Acoustics* (to appear in 1997, Vol. 119). Free vibrations of thick hollow circular cylinders from three-dimensional analysis.
4. A. W. LEISSA and J. SO 1995 *Journal of Vibration and Control* **1**, 145–158. Three-dimensional vibrations of truncated hollow cones.
5. J. SO 1993 *Ph.D. Dissertation*, *The Ohio State University*. Three-dimensional vibration analysis of elastic bodies of revolution.
6. J. R. HUTCHINSON 1984 *Journal of Applied Mechanics* **51**, 581–585. Vibration of thick free circular plates, exact versus approximate solutions.
7. J. R. HUTCHINSON and S. A. EL-AZHARI 1986 *Refined Dynamical Theories of Beams*, *Plates*, *and Shells and Their Applications*, *Proceedings of the Euromech-Colloquium* **219**, 102–111. On the vibration of thick annular plates.
8. M. ENDO 1972 *Bulletin of JSME* **15**, 446–454. Flexural vibrations of a ring with arbitrary cross section.
9. R. K. SINGAL and K. WILLIAMS 1988 *Journal of Vibration*, *Acoustics*, *Stress*, *and Reliability in Design* **110**, 533–537. A theoretical and experimental study of vibrations of thick circular cylindrical shells and rings.
10. R. D. MINDLIN 1955 *Journal of Applied Mechanics* **18**, 31–38. Influence of rotary inertia and shear on flexural motions of isotropic, elastic plates.
11. H. DERESIEWICZ and R. D. MINDLIN 1955 *Journal of Applied Mechanics* **22**, 86–88. Axially symmetric flexural vibrations of isotropic elastic plates.
12. H. DERESIEWICZ and R. D. MINDLIN 1954 *Journal of Applied Physics* **25**, 1329–1332. Thickness shear and flexural vibrations of a circular disk.

13. T. Irie, G. Yamada and S. Aomura 1980 *Journal of Applied Mechancis* **47**, 652–655. Natural frequencies of Mindlin circular plates.
14. A. W. Leissa 1993 *Acoustical Society of America*, *Originally issued by NASA* 1973, 11–12, Vibration of plates.
15. G. M. L. Gladwell and D. K. Vijay 1975 *Journal of Sound and Vibration* **42**, 387–397. Natural frequencies of free finite length circular cylinders.
16. J. R. Hutchinson 1995 *Journal of Applied Mechanics* **62**, 818–819. Vibrations of solid cylinders revisited.